Environ. Sci. Technol. **1997**, *31*, 1754−1760

Photoisomerization Kinetics of Stilbene-Type Fluorescent Whitening Agents

SILVIO CANONICA* AND JOHANNES B. KRAMER

Swiss Federal Institute for Environmental Science and Technology (EAWAG) and Swiss Federal Institute of Technology (ETH), CH-8600 Dübendorf, Switzerland

DANIEL REISS AND HANSRUEDI GYGAX†

Physical Chemistry Laboratory, Swiss Federal Institute of Technology, ETH Zentrum, CH-8092 Zürich, Switzerland

Photoisomerization of stilbene-type fluorescent whitening agents (FWAs) is an important process that governs their isomer distributions and photodegradation rates in the aquatic environment. Kinetic expressions relating parameters for singlet excited-state dynamics, photoisomerization, and photodegradation were derived. Picosecond time-correlated single photon counting and stationary monochromatic irradiation were used to study the fluorescence lifetimes and steady-state isomer ratios of three widely used FWAs in aqueous solution. Fluorescence lifetimes decrease and *Z*/*E*-isomer ratios increase with increasing temperature, which can be interpreted in terms of an activated rate process in the first excited singlet state of the *E*-isomer having an activation energy of 20−26 kJ mol^{-1}. The data obtained in the laboratory enable prediction of the FWAs isomer distributions as a function of temperature and under various irradiation conditions in sunlit freshwaters.

Introduction

Fluorescent whitening agents (FWAs) are largely used in textile and paper manufacturing and in household detergents. Detergent use, in particular, causes thousands of tons per year (*1*, *2*) of these compounds to be discharged into sewage treatment plants or directly into the aquatic environment worldwide. FWAs are not readily biodegradable (*1*, *3*) and the major sink in the environment is possibly direct photodegradation by sunlight in surface waters. In a recent study (*4*), we reported that the photodegradation quantum yields of three widely used stilbene-type FWAs (Figure 1) are small ($\approx 10^{-4}$); however, due to the strong absorption band of the FWAs in the UV-A spectral range, their photodegradation half-lives at the surface of sunlit natural waters may be shorter than 5 h. The rate constants for photodegradation were found to be strongly influenced by a fast photoisomerization that, depending on molecular parameters and irradiation conditions, determined the rate of light absorption by the isomer mixture. Photoisomerization of FWAs was also found to control their partitioning between aqueous solution and suspended solids in sewage treatment plants and rivers (*5*).

Like many stilbene derivatives, stilbene-type FWAs can undergo reversible photoisomerization due to twisting about the stilbene double bond. Thermal isomerization can be neglected because of the high energy barrier between the *E*- and *Z*-isomers in their electronic ground state (*6*). The rate of photoisomerization as well as the fluorescence quantum yield, position of isomer equilibrium, and rate of photodegradation are strongly dependent on the environment of the molecules. All FWAs have high fluorescence quantum yields (>0.9) on cotton (*7*) that become lower in solution (*8*). In aqueous solution, photoisomerization from the fluorescent *E*- (or *trans*-) isomer, which is the active FWA, takes place at quantum yields in the range $\approx 10^{-2}-10^{-1}$ (*8*), whereas photoisomerization from the non-fluorescent *Z*- (or *cis*-) isomer is expected to have a quantum yield of roughly 0.5 (vide infra). Since the quantum yield for photoisomerization is at least 2 orders of magnitude higher than for photodegradation, a photostationary isomer equilibrium is maintained during the course of photodegradation (*4*). This gives rise to pseudo-first-order kinetics for photodegradation at constant irradiation intensity. In the theoretical section of this paper, we describe the relations between quantum yields and rate constants for the different photoprocesses involved under mono- and polychromatic irradiation conditions. These equations are of general validity for describing photodegradation processes in the presence of rapid photoisomerization, as expected for other photoactive substances such as several azo compounds (*9*).

In this study, we further investigate the water solution photophysics and photochemistry of the three FWAs described in Figure 1 by measuring their fluorescence lifetimes and photoisomer distributions at various temperatures in the range 5−45 °C. These data allow us to extract the parameters controlling the temperature dependence of the ratio of *E*/*Z* to *Z*/*E* photoisomerization quantum yields, which are used to predict isomer distributions in sunlit natural waters.

Theory

Singlet Excited-State Dynamics of Stilbenes. Photoisomerization dynamics of stilbenes in solution is commonly described using the twisting angle about the double bond linking the two phenyl moieties as the only reaction coordinate (*10*−*12*). Twisting in the first excited singlet state is supposed to proceed adiabatically from the *E*- as well as the *Z*-isomer to an intermediate conformation at an angle of about 90°, from where rapid relaxation (∼1 ps) to the ground-state potential energy curve takes place (Figure 2). Isomerization of the first excited singlet (*E*)-stilbene is hindered by a solvent-dependent activation barrier, which decreases from 14.7 kJ mol^{-1} in alkane solvents to estimated values of <4 kJ mol^{-1} in alkyl alcohol solvents (*11*). The other pathway, isomerization of the first excited singlet (*Z*)-stilbene, is considered to be barrierless. Recently, it has been shown that a small barrier (<4.6 kJ mol^{-1}) might be present in alkane solutions (*13*), but this should become negligible in polar solvents. The much higher barrier in the potential energy curve of the singlet excited *E*-isomer can explain why (*E*)-stilbene and many of its derivatives, such as the *E*-FWAs, have much higher fluorescence quantum yields than the corresponding *Z*-isomers. Solvent viscosity is also an important factor that controls the rate of twisting about the double bond. An empirical expression of the following form has been widely used for fitting twisting (or isomerization) rate coefficients k_E^{tw} from the first excited singlet *E*-isomer (*11*):

$$k_E^{tw} = \frac{A}{\eta^B} \exp(-E_E^{act}/RT) \qquad (1)$$

* Corresponding author telephone: +411 823 5453; fax: +411 823 5471; e-mail address: canonica@eawag.ch.

† Present address: Givaudan-Roure Forschung AG, RSM, Ueberlandstrasse 138, CH-8600 Dübendorf, Switzerland.

S0013-936X(96)00748-1 CCC: $14.00 © 1997 American Chemical Society

DSBP

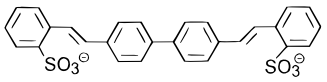

4,4'-bis(2-sulfostyryl)biphenyl

DAS 1

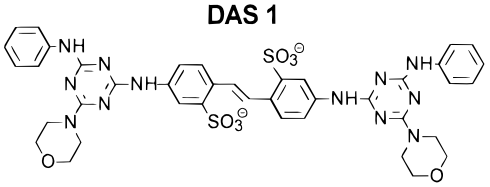

4,4'-bis[(4-anilino-6-morpholino-1,3,5-triazin-2-yl)amino]stilbene-2,2'-disulfonate

DAS 2

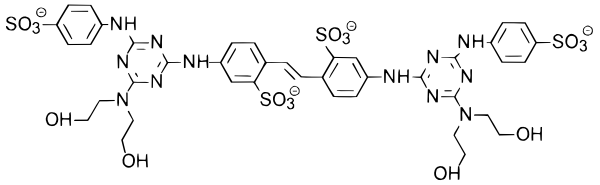

4,4'-bis[(4-(4-sulfoanilino)-6-bis(2-hydroxyehtyl)amino-1,3,5-triazin-2-yl)amino]stilbene-2,2'-disulfonate

FIGURE 1. Structures and names of the FWAs.

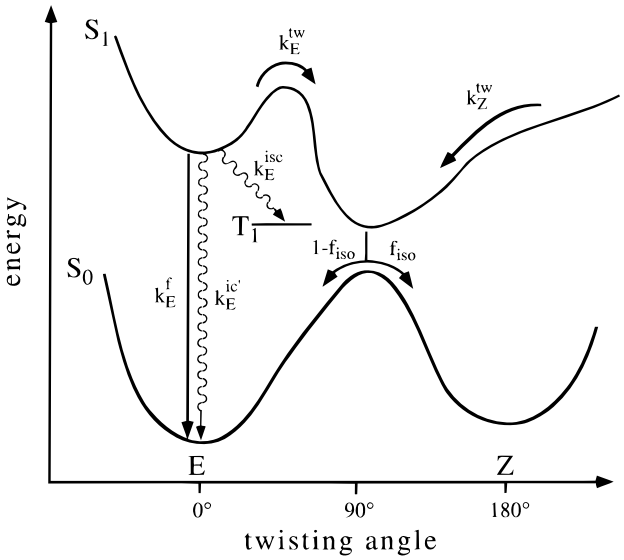

FIGURE 2. Processes involved in the photoisomerization of singlet excited stilbenes.

where A and B ($0 \le B \le 1$) are fitting parameters, η is solvent viscosity, R is the universal gas constant, T is temperature, and E_E^{act} is the activation energy, a parameter that can be determined in some cases from isoviscosity plots. For alcohol solvents, however, determination of E_E^{act} is unreliable, and this should apply also to water. For the present application, water is the only solvent used, and hence it is more practical to use a simple Arrhenius expression:

$$k_E^{tw} = A \exp(-E_E/RT) \tag{2}$$

where E_E is an empirical activation energy that also includes viscosity effects. The relaxation coefficient for the singlet excited E-isomer, which is the inverse of the fluorescence

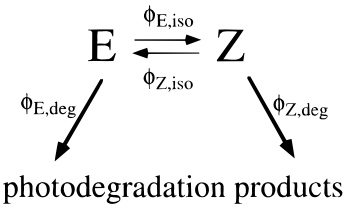

FIGURE 3. Kinetic scheme including photoisomerization and photodegradation of the FWAs.

lifetime τ_E^{S1}, can be expressed as:

$$k_E^{S1} = k_E^f + k_E^{ic'} + k_E^{isc} + k_E^{tw} = (\tau_E^{S1})^{-1} \tag{3}$$

where the k_E values are the relaxation coefficients and the superscripts refer to the different relaxation channels: f ≡ fluorescence; ic′ ≡ internal conversion, excluding twisting; isc ≡ intersystem crossing to the triplet manifold. With respect to the model commonly used for stilbene (*8*, *11*), we allow for two additional radiationless relaxation channels other than twisting, characterized by $k_E^{ic'}$ and k_E^{isc}. These may be effective for the FWAs, as they were shown to be for stilbenes bearing various substituents (*12*, *14*). As a first approximation, only k_E^{tw} can be considered to be temperature- and viscosity-dependent, and the other coefficients gathered to give the constant k_E^1:

$$k_E^1 = k_E^f + k_E^{ic'} + k_E^{isc} \tag{4}$$

Combining eqs 2 and 4, the following temperature dependence for the singlet state relaxation coefficient is obtained:

$$k_E^{S1}(T) = k_E^1 + A \exp(-E_E/RT) \tag{5}$$

Quantum Yields and Rate Constants for Phototransformations. The photochemistry of stilbene derivatives like the FWAs considered in this study may be represented by the kinetic scheme in Figure 3. Each quantum yield ϕ can be associated with a first-order rate coefficient $k_{X,i}$ describing a given transformation, i, of each isomer, X, with respect to its concentration in the electronic ground state. For monochromatic irradiations and optically thin solutions, we use the expression:

$$k_{X,i}(\lambda) = 2.303\, I(\lambda)\epsilon_X(\lambda)\phi_{X,i}(\lambda) \tag{6}$$

where $\epsilon_X(\lambda)$ is the (decadic) extinction coefficient of the isomer X and $I(\lambda)$ is the photon fluence rate. In the following treatment, we assume the quantum yields $\phi_{X,i}$ to be independent of wavelength, a condition that should hold for the FWAs since only one absorption band plays a significant role for sunlight absorption. As already mentioned, the E- and Z-isomers of each FWA may be considered to be at photostationary equilibrium on the photodegradation time scale, with the time-independent isomer ratio $\alpha_{EZ}(\lambda)$ given by

$$\alpha_{EZ}(\lambda) = \frac{[Z]_{ps}}{[E]_{ps}}(\lambda) = \frac{k_{E,iso}(\lambda)}{k_{Z,iso}(\lambda)} = \frac{\epsilon_E(\lambda)\phi_{E,iso}}{\epsilon_Z(\lambda)\phi_{Z,iso}} \tag{7}$$

On the time scale of degradation, it is not possible to distinguish which of the isomers reacts at which rate. The expression for the photodegradation rate coefficient of a given isomer mixture is

$$k_{\alpha,deg}(\lambda) = 2.303 I(\lambda)\, \epsilon_\alpha(\lambda)\phi_{\alpha,deg} \tag{8}$$

where $\epsilon_\alpha(\lambda)$ is the extinction coefficient of the isomer mixture, defined as (*4*)

$$\epsilon_\alpha(\lambda) = \frac{\epsilon_E(\lambda) + \alpha_{EZ}(\lambda)\epsilon_Z(\lambda)}{1 + \alpha_{EZ}(\lambda)} \quad (9)$$

and $\phi_{\alpha,deg}$ is the quantum yield for the isomer mixture. By simple kinetic considerations and assuming the photostationary isomer equilibrium to be maintained, the following equation can be derived:

$$k_{\alpha,deg}(\lambda) = \frac{k_{E,deg}(\lambda) + \alpha_{EZ}(\lambda)k_{Z,deg}(\lambda)}{1 + \alpha_{EZ}(\lambda)} \quad (10)$$

Combining eqs 8−10 and expressing the photodegradation rate coefficients by eq 6 yields

$$\phi_{\alpha,deg} = \frac{\epsilon_E(\lambda)\phi_{E,deg} + \alpha_{EZ}(\lambda)\epsilon_Z(\lambda)\phi_{Z,deg}}{\epsilon_E(\lambda) + \alpha_{EZ}(\lambda)\epsilon_Z(\lambda)} \quad (11)$$

which, by using eq 7, can be transformed into

$$\phi_{\alpha,deg} = \frac{\phi_{E,deg} + \frac{\phi_{E,iso}}{\phi_{Z,iso}}\phi_{Z,deg}}{1 + \frac{\phi_{E,iso}}{\phi_{Z,iso}}} \quad (12)$$

Thus, the quantum yield for the photodegradation of the isomer mixture at photostationary equilibrium is independent of $\alpha_{EZ}(\lambda)$. It is only a function of the quantum yields for the different photoprocesses involved, which in turn can also be assumed to be independent of λ. From eq 12, it can also be concluded that the ratio of the photoisomerization quantum yields, $\phi_{E,iso}/\phi_{Z,iso}$, controls the contribution of each isomer to the degradation quantum yield of the isomer mixture.

Using broadband irradiation, as is the case for sunlight, α_{EZ} is no longer given by eq 7 but has to be expressed as

$$\alpha_{EZ} = \frac{[Z]_{ps}}{[E]_{ps}} = \frac{\phi_{E,iso}}{\phi_{Z,iso}} \frac{\int \frac{dI(\lambda)}{d\lambda}\epsilon_E(\lambda)\, d\lambda}{\int \frac{dI(\lambda)}{d\lambda}\epsilon_Z(\lambda)\, d\lambda} \quad (13)$$

where $dI(\lambda)/d\lambda$ is the spectral density of the photon fluence rate. As for monochromatic irradiation, it can be shown that $\phi_{\alpha,deg}$ can be described by eq 12. The photodegradation rate coefficient is calculated numerically using the expression:

$$k_{\alpha,deg} = 2.303\phi_{\alpha,deg}\int \frac{dI(\lambda)}{d\lambda}\epsilon_\alpha(\lambda)\, d\lambda \quad (14)$$

where $\epsilon_\alpha(\lambda)$ is obtained by using eq 9 with α_{EZ} (measured or calculated from eq 13) instead of $\alpha_{EZ}(\lambda)$.

Relation between Singlet Excited-State Relaxation Parameters and Photostationary Isomer Distributions. We define the efficiency of formation of the *Z*-isomer in the ground state from the excited twisted configuration at ~90° as f_{iso} [see Figure 2; this efficiency is also called the branching ratio (*8*)] and express the quantum yield for *E*/*Z*-photoisomerization as

$$\phi_{E,iso} = \frac{k_E^{tw} f_{iso}}{k_E^1 + k_E^{tw}} = k_E^{tw}\tau_E^{S1} f_{iso} \quad (15)$$

The efficiency of formation of the excited twisted configuration from the excited *Z*-isomer can be assumed to be unity, because relaxation due to twisting should be much faster than all other processes. The formation of dihydrophenanthrenes, which is known to occur from the excited *E*-isomer in the case of stilbene (*15*), could not be detected in this or previous studies on FWAs (*4, 5*) and was therefore neglected. Thus, the quantum yield for *Z*/*E*-photoisomerization is

$$\phi_{Z,iso} = 1 - f_{iso} \quad (16)$$

Combining eqs 15 and 16 gives

$$\frac{\phi_{E,iso}}{\phi_{Z,iso}} \frac{1}{\tau_E^{S1}} = \frac{f_{iso}}{1 - f_{iso}} k_E^{tw} \quad (17)$$

Experimental Section

Materials and Solutions. The FWAs DSBP [4,4′-bis(2-sulfostyryl)biphenyl], DAS 1 [4,4′-bis[(4-anilino-6-morpholino-1,3,5-triazin-2-yl)amino]stilbene-2,2′-disulfonate], and DAS 2 [4,4′-bis[(4-(4-sulfoanilino)-6-bis(2-hydroxyethyl)amino-1,3,5-triazin-2-yl)amino]stilbene-2,2′-disulfonate] (see Figure 1) were supplied as sodium salts by Ciba-Geigy AG (Basel, Switzerland). Other chemicals were analysis grade from common commercial sources. All chemicals were used as received. FWA sample solutions were made by diluting stock solutions (250 μM) in bidistilled water buffered at pH 8.0 with 0.05 M phosphate.

Picosecond Time-Correlated Single Photon Counting for Determining Fluorescence Lifetimes. Time-resolved fluorescence experiments were performed using a typical arrangement for time-correlated single photon counting (TCSPC) (*16*). The excitation source consists of a mode-locked frequency-doubled Coherent Antares Nd:YAG Laser system and a synchronously pumped extended sulforhodamine B dye laser. The output was a periodic train of 10 ps fwhm pulses with a separation of 13.22 ns and an average power of about 300 mW at 642 nm. After generation of the second harmonic by means of a Spectra Physics 390 frequency doubler, an average power of about 4 mW at 321 nm was obtained. The emission from the sample was analyzed by a Spex 1400 double monochromator, which was modified for subtractive dispersion, and imaged on a Hamamatsu R 1564U-07 microchannel plate photomultiplier (MCP). The MCP output signal was amplified using a B&H 3002-DC 3.1 GHz preamplifier, inverted with an AVTECH Electro Systems AVX-2 inverting transformer, and valid pulses were selected by an Ortec 9307 Picotiming discriminator to be used as start signal for the electronic clock. The timing reference signal was taken from a Spectra Physics 403 B fast photodiode, amplified by an HP 8447F 0.1-1300 MHz amplifier. The electronic clock, an Ortec 467 time-to-amplitude converter (TAC), was used in the so-called reverse mode, whereby the time difference between a detected photon (start) and the reference signal (stop) was measured. The TAC output was directed to a Silena 7423 UHS analog to digital converter, and the events were stored as a histogram in a Silena 7328/S-8K memory buffer unit and transferred via an IEEE-488 interface (GPIB) to a SUN SPARC II workstation. With this setup, one can achieve apparatus response functions as short as 80 ps fwhm. Analysis of the fluorescence decay curve to obtain fluorescence lifetimes was performed by deconvolution in the Fourier space (*17*). To minimize intensity losses and other side effects due to photoisomerization, 3 μM solutions of the *E*- or *E*,*E*-isomers of the FWAs were pumped through a 100-μL fluorescence flow cell (Hellma Model 176.171-QS) at a flow rate of about 20 mL/min. Sample solutions, contained in a 100-mL amber glass bottle reservoir, and cell holder were thermostated at the same temperature.

Stationary Irradiation and Measurement of Steady-State Photoisomer Distributions. A photoirradiation system from Applied Photophysics (London, U.K.), consisting of a 900-W xenon source and an f/3.4 grating monochromator, was used for stationary irradiations. DSBP was irradiated at 370 nm; DAS 1 and DAS 2 were irradiated at 320 nm. The optical band width was 23 nm for all experiments. The samples (FWA concentration, 1 μM) were contained in a quartz glass

TABLE 1. Summary of Experimental Data in Temperature Range 5−45 °C

	fluorescence lifetimes (ns)			photoisomerization quantum yield ratios $\phi_{E,iso}/\phi_{Z,iso}$		
T (°C)	(*E,E*)-DSBP	(*E*)-DAS-1	(*E*)-DAS-2	DSBP	DAS 1	DAS 2
5.0	1.42	0.65	0.69	0.089	0.527[a]	0.490
25.0	1.27	0.47	0.52	0.136	0.804	0.768
45.0	1.20	0.35	0.38	0.229	1.069	0.907

[a] At 6.3 °C.

cuvette (volume, 3 mL), which was placed in a temperature-regulated holder, and stirred magnetically during irradiation. Temperature was measured directly in the sample solution (accuracy ±0.2 K). Samples were taken at three different delay times to check whether the photostationary distribution had been reached. All samples were analyzed by reverse-phase HPLC using a Hewlett Packard 1050 system equipped with quaternary gradient pump and variable wavelength UV detector. The analysis method has been described in detail elsewhere (*4*). Concentrations of the *E*- and *E,E*-isomer ([E] and [E,E], respectively) were determined by comparison with a pure non-irradiated standard of the same isomer, $[E]_0$ or $[E,E]_0$, which also served as a starting material for irradiations. Concentrations of the *Z*- and *E,Z*-isomer were calculated by the subtraction $[E]_0 - [E]$ and $[E,Z]_0 - [E,Z]$, respectively. The concentration of (*Z,Z*)-DSBP was always negligible, and therefore the processes of *E,Z*/*Z,Z*- and *Z,Z*/*E,Z*-photoisomerization were neglected. The equations derived in the previous section were also used for DSBP, the index "E" denoting the *E,E*-isomer and the index "Z" denoting the *E,Z*-isomer.

Relative fluorescence quantum yields of the *E*-isomers of the FWAs (2.5 μM solutions) were determined using a Shimadzu RF-551 spectrofluorometric detector (band width 15 nm) with excitation wavelength at 350 nm and integrating the fluorescence spectrum from 380 to 540 nm at 5-nm intervals. The excitation light beam was attenuated 1:10 using a neutral-density filter, and the sample was pumped through the 100-μL flow cell (see above) at a flow rate of 40−50 mL/min to avoid a decrease in fluorescence intensity due to photoisomerization.

Results and Discussion

Fluorescence Lifetimes. In most cases, the fitting of the fluorescence decay curves to a sum of two exponential functions leads to more accurate results than using one exponential. The lifetime of the major exponential component, which was assigned to the fluorescence of the FWA, was associated with a normalized pre-exponential factor of at least 0.99. The minor exponential component was possibly due to noise of the detection system or impurities in the solution of FWAs.

The fluorescence lifetimes of the three FWAs decrease with increasing temperature (Table 1). The *E*-isomers of the two diaminostilbene dyes have almost identical fluorescence lifetimes, differing by less than 12% over the whole temperature range and decreasing by about 45% in going from 5 to 45 °C. In contrast, the fluorescence lifetime of (*E,E*)-DSBP is a factor of 2−3 times longer than that of (*E*)-DAS 1 and (*E*)-DAS 2 and has a weaker temperature dependence. The radiative constant k_E^f could be calculated by using the fluorescence quantum yield values at 25 °C: 0.82 for (*E,E*)-DSBP (*8*), 0.33 for (*E*)-DAS 1, and 0.35 for (*E*)-DAS 2 (relative quantum yields determined in this work, taking DSBP as a standard). Assuming all non-radiative relaxation channels, with the exception of twisting (tw), to be ineffective, k_E^1 ($\approx k_E^f$) and k_E^{tw} could be calculated. Under this assumption (denoted method A), the Arrhenius activation energies using

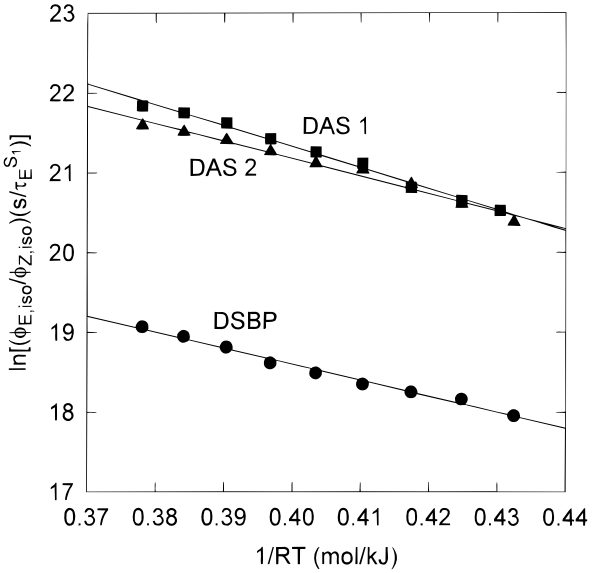

FIGURE 4. Arrhenius plots (eq 18, method B) for the fluorescence lifetimes combined with the photoisomerization quantum yield ratios.

eq 2 give 17.9 ± 6.3 kJ mol^{-1} for DSBP, 18.8 ± 1.5 kJ mol^{-1} for DAS 1, and 17.6 ± 1.0 kJ mol^{-1} for DAS 2 (the errors indicate 95% confidence intervals from linear regression of ln k_E^{tw} versus 1/*RT*). These activation energies are very low and are close to the activation energy of the viscosity of water in the same temperature range (17.4 kJ mol^{-1}) and the value of 17.8 kJ mol^{-1} obtained for a DAS type FWA using the same assumption but an alternative experimental method (*8*).

Steady-State Photoisomer Distributions. From the experimentally determined steady-state concentration values of the photoisomers, using eq 7 and correcting for the finite band width of the monochromator used for irradiation, the ratio $\phi_{E,iso}/\phi_{Z,iso}$ at various temperatures was obtained (Table 1). The values of λ used for irradiating the samples were chosen in order to give stationary concentrations of both isomers in the same order of magnitude, which minimizes the experimental error in the determination of the photoisomerization quantum yield ratio. The accuracy of $\phi_{E,iso}/\phi_{Z,iso}$ also depends on the accuracy of the extinction coefficients used in the calculation. Relative errors in the ϵ values were estimated to be less than 5% for DSBP and DAS 1, but could be as high as 15% for DAS 2, which was available in a less pure form. Over the temperature range investigated, $\phi_{E,iso}/\phi_{Z,iso}$ increases by a factor of 2−3 with increasing temperature for all FWAs studied.

Using both experimentally determined fluorescence lifetimes and photoisomerization quantum yield ratios, it is possible to obtain the activation energy E_E, which describes the temperature dependence of k_E^{tw}. Combining eqs 2 and 17, one can derive the following Arrhenius-type equation:

$$\ln\left[\frac{\phi_{E,iso}}{\phi_{Z,iso}}\frac{1}{\tau_E^{S1}}\right] = \ln\left[\frac{f_{iso}}{1-f_{iso}}A\right] - E_E/RT \qquad (18)$$

Such Arrhenius plots (denoted method B) are shown in Figure 4 and yield the E_E values given in Table 2. Note that eq 18 does not include the restrictive assumption made using method A (i.e., $k_E^1 \approx k_E^f$). These activation energies are higher than the activation energy of solvent viscosity (17.4 kJ mol^{-1}). With the exception of DSBP, they are also significantly higher than the activation energies obtained by method A. The E_E values in Table 2 were used to estimate k_E^1 and the preexponential factor *A* in eq 5 (Figure 5 and Table 2). The best-fit parameters from eqs 18 and 5 could be used to calculate f_{iso} and other useful parameters, which are also given in Table 2. Parameter values very close to those of Table 2 were also

TABLE 2. Kinetic Parameters for Photoisomerization of FWAs

	DSBP	DAS-1	DAS-2
E_E (kJ mol^{-1})[a]	20.1 ± 1.8	26.4 ± 2.1	22.0 ± 2.6
k_E^1 (s^{-1})[b]	(6.7 ± 0.3) × 10^8	(1.13 ± 0.15) × 10^9	(9.5 ± 0.9) × 10^8
A (s^{-1})[b]	(3.3 ± 1.0) × 10^{11}	(3.9 ± 0.5) × 10^{13}	(7.1 ± 0.6) × 10^{12}
k_E^{tw} (25 °C) (s^{-1})[c]	1.02 × 10^8	9.4 × 10^8	1.00 × 10^9
ϕ_E^{tw} (25 °C)[d]	0.13	0.46	0.51
f_{iso}[e]	0.52	0.64	0.60
$\phi_{E,iso}$ (25 °C)[f]	0.069	0.29	0.31

[a] From linear regression using eq 18. [b] From linear regression using eq 5. [c] Calculated using eq 5. [d] k_E^{tw} (25 °C)/k_E^{S1}. [e] Average from eq 17 using experimental values for $\phi_{E,iso}/\phi_{Z,iso}$ and τ_E^{S1} and calculated k_E^{tw} (see footnote c) at different temperatures. [f] ϕ_E^{tw} (25 °C)f_{iso}.

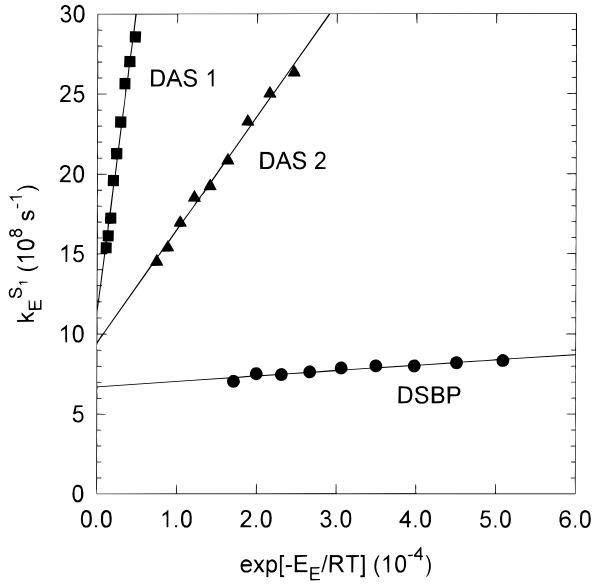

FIGURE 5. Linear regressions of the inverse fluorescence lifetimes according to eq 5.

obtained by simultaneously fitting the experimental fluorescence lifetimes and photoisomerization quantum yield ratios to eqs 5 and 17 using a non-linear least-square regression (see Supporting Information for details). This confirms that method B, which consists of two successive linear regression steps, is a valid fitting procedure.

Photoisomerization Mechanisms. The k_E^1 value for DSBP (6.7 × 10^8 s^{-1}) is very close to the value of k_E^f (6.9 × 10^8 s^{-1}) obtained from fluorescence lifetime and quantum yield data (*8*), indicating that relaxation pathways of the excited singlet *E*,*E*-isomer other than the temperature-dependent process should be negligible. The observed temperature dependence, however, can hardly be associated with that of a singlet state process (k_E^{tw}) for two principal reasons:

(a) The frequency factor *A* (Table 2) appears to be too low—for an excited singlet process of various substituted stilbenes it was found to be 10^{12}–10^{13} s^{-1} (*14*), i.e., about 1 order of magnitude higher than the experimental value for DSBP.

(b) k_E^{tw} (Table 2) for DSBP is about 9 times smaller than k_E^{tw} for DAS 1 or DAS 2—it is expected to be higher because the activation energy for DSBP is somewhat lower than the activation energy for the other two FWAs and the viscous drag on the twisting group about the C–C double bond is much smaller for DSBP than for the DAS type FWAs, which carry bulky substituents.

The photoisomerization of (*E*,*E*)-DSBP might be interpreted in terms of an activated intersystem crossing, which determines the temperature dependence of the fluorescence lifetime and the steady-state photoisomer concentration ratio, followed by isomerization in the triplet state. Oxygen at concentrations up to those valid for air-saturated water should have no measurable effect on such intersystem crossing. This hypothesis also implies that the activation barrier (including friction) to isomerization in the first excited singlet state of (*E*,*E*)-DSBP should be much higher than 20 kJ mol^{-1}. This effect on the excited singlet potential surface could be due to the biphenyl moiety. Alternatively, photoisomerization could take place after photoionization with subsequent formation of DSBP radical cations, which were probably among the transients observed after laser flash photolysis of DSBP (*18*).

For both DAS 1 and DAS 2, the mechanism depicted in Figure 1 can account for the experimental data. Assuming this scheme is correct, radiationless relaxation pathways from the excited singlet *E*-isomer other than twisting toward the 90° conformation should be important. From the k_E^1 values of Table 2 and the radiative constant k_E^f obtained from fluorescence lifetimes and quantum yields, $k_E^{ic'} + k_E^{isc}$ values of 4.3 × 10^8 s^{-1} for DAS 1 and 2.8 × 10^8 s^{-1} for DAS 2 were calculated (eq 4). The experimental methods used here do not allow us to distinguish between intersystem crossing and internal conversion. These additional radiationless deactivation channels could be promoted by a limited torsion of the excited singlet *E*-isomer about the C–C double bond, which would be allowed since the bulky substituents at the double bond are highly flexible.

Phototransformations of FWAs in Sunlit Freshwaters. Parameters characterizing the photostationary isomer distributions under clear-sky radiation are given in Table 3. They were calculated using the $\phi_{E,iso}$ and $\phi_{Z,iso}$ values for $T = 25$ °C (from Table 2) and the computer program GCSOLAR (*19*), which computes rate constants for phototransformations in natural waters. The very short times for >99% relaxation [these correspond to five times the relaxation times, given by $(k_{E,iso} + k_{Z,iso})^{-1}$] indicate that in the photic zone of natural waters FWAs may be considered at the photostationary state established by daylight. Equation 13 is the key for calculating α_{EZ} and therefore the isomer distribution of the FWAs at the photostationary state under sunlight irradiation. The right-hand side of eq 13 consists of two terms: the temperature-dependent ratio of the photoisomerization quantum yields ($\phi_{E,iso}/\phi_{Z,iso}$) determined above and the integral term representing the ratio of the rates of light absorption by each of the isomers. The second term varies depending on irradiation conditions. Calculated isomer distributions of DSBP and DAS 1 for the surface of a water body are in very good agreement with those measured during the course of a photodegradation experiment using sunlight (*4*). The slightly larger deviation observed for DAS 2 is probably due to uncertainties in the determination of the absorption spectra. The data in Table 3 show that the DAS-type FWAs are mainly present in their *Z*-isomer. In contrast, when these compounds are adsorbed on cotton, the *E*-isomer is predominant at the photostationary state under sunlight irradiation [the fraction of (*E*)-DAS 1 was determined to be >90% on cotton (*7*)].

The actual isomer distribution in the photic zone of natural waters can deviate from the surface values, because shorter wavelengths are generally absorbed more strongly by the waters (*20*). This favors the *E*/*Z*-isomerization [the *E*- and *E*,*E*-isomers absorb more at longer wavelength than the *Z*- and *E*,*Z*-isomers (*4*)] and causes α_{EZ} to increase with increasing depth. Simulations done using the absorption spectrum of water from Greifensee, a eutrophic Swiss lake, show that the fractions of *E*- and *E*,*E*-isomers in the photic zone decrease a few percent from surface values. Table 3 also illustrates that solar altitude, which changes daily and yearly, can slightly affect the isomer distribution. Figure 6 shows that despite the pronounced temperature dependence of $\phi_{E,iso}/\phi_{Z,iso}$, the

TABLE 3. Simulations for FWAs Photoisomerization in Lake Water[a] (T = 25 °C)

FWA	solar altitude (deg)	surface layer depth (m)	$k_{E,iso}$ (s^{-1})	$k_{Z,iso}$ (s^{-1})	$5\tau_r$[b] (s)	α_{EZ}	% *E*- or *E,E*-isomer
DSBP	60	0	1.22×10^{-1}	5.04×10^{-1}	8	0.242	80.5
		5	7.78×10^{-3}	2.74×10^{-2}	142	0.284	77.9
	5	0	7.00×10^{-3}	2.49×10^{-2}	157	0.281	78.1
		5	4.56×10^{-4}	1.41×10^{-3}	2680	0.323	75.6
DAS 1	60	0	5.05×10^{-1}	8.13×10^{-2}	9	6.212	13.9
		5	3.71×10^{-2}	3.90×10^{-3}	122	9.513	9.5
	5	0	3.01×10^{-2}	3.35×10^{-3}	149	8.985	10.0
		5	2.25×10^{-3}	1.73×10^{-4}	2064	13.006	7.1
DAS 2	60	0	5.81×10^{-1}	1.26×10^{-1}	7	4.611	17.8
		5	4.10×10^{-2}	6.31×10^{-3}	106	6.498	13.3
	5	0	3.46×10^{-2}	5.45×10^{-3}	125	6.349	13.6
		5	2.49×10^{-3}	2.97×10^{-4}	1794	8.384	10.7

[a] Water from Greifensee (see text). Absorption spectrum of filtered water used in the calculations. [b] Relaxation time for reaching the photostationary state: $\tau_r = (k_{E,iso} + k_{Z,iso})^{-1}$.

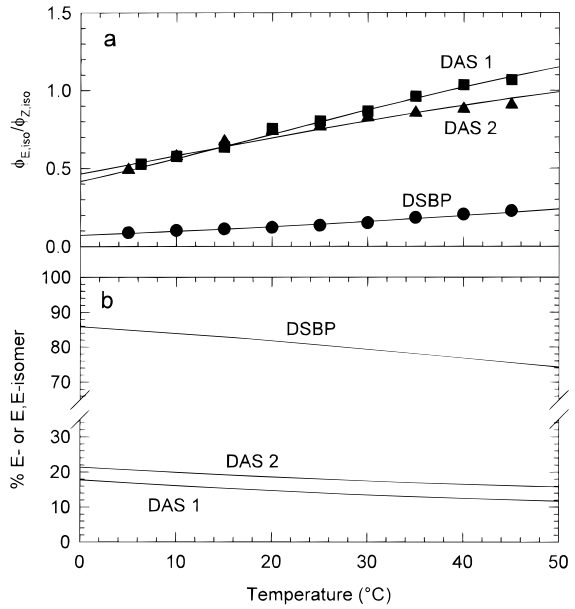

FIGURE 6. Temperature dependence of (a) the photoisomerization quantum yield ratios (lines are data fits according to eqs 15 and 16 using the parameters in Table 2) and (b) the fraction of *E*- or *E,E*-isomer calculated for summer noon sunlight irradiation at the surface of a water body.

fractions of *E*- and *E,E*- isomers of the FWAs decrease only slightly with increasing temperature. In conclusion, for a precise prediction of isomer distributions at the photostationary state in freshwaters, the temperature, absorption, and irradiation conditions of the water body must be taken into account. However, considering typical variations of these parameters in freshwaters, *E*- and *E,E*-isomer fractions are expected to vary in a relatively narrow range (75−86% for DSBP, 7−18% for DAS 1, and 11−21% for DAS 2).

Since the *E*- and *E,E*-isomers of the FWAs generally adsorb much more readily to particles than the corresponding *Z*- and *E,Z*-isomers (*5*), the transport of FWAs in natural waters may be strongly dependent on whether they had been in contact with sunlight. This should be particularly important for DAS 1 because of its higher affinity for surfaces as compared to the other two FWAs. Thus, in the presence of high particle concentrations during a dark period, the fractions of dissolved *E*- and *E,E*-isomers may be reduced with respect to their solution photostationary state value. In the presence of light at high particle concentration, fast adsorption and desorption and photoisomerization of adsorbed FWAs are expected to affect their isomer distribution.

As seen in the theoretical section, photoisomerization quantum yields and isomer distributions at the photostationary state affect the rates of photodegradation of the FWAs. Equation 14 was used successfully in our previous paper to calculate photodegradation rate coefficients under natural sunlight, summer noon irradiation conditions (*4*). The molar extinction coefficient of the isomer mixture in the solar UV spectral region increases with increasing fraction of *E*- or *E,E*-isomer. The ranges of isomer fractions given above, which consider temperature and spectral changes, give rise to the following variability of the integral in eq 14 (assuming constant fluence rate): 3% for DSBP, 30% for DAS 1, and 30% for DAS 2. Equation 12 describes the dependence of $\phi_{\alpha,deg}$ on $\phi_{E,iso}/\phi_{Z,iso}$. However, without knowledge of $\phi_{E,deg}$ and $\phi_{Z,deg}$, which are not experimentally available for the FWAs studied here, it is not possible to predict the temperature dependence of $\phi_{\alpha,deg}$ on the basis of the temperature dependence of $\phi_{E,iso}/\phi_{Z,iso}$.

The methods used in this study could be equally applied to the transformation of other pollutants or natural compounds exhibiting fast reversible photoisomerization. Attention must be paid to possible complications arising from fast competing thermal isomerization processes or from a wavelength dependence of the photochemical quantum yields. A kinetic treatment similar to the one used here might also be useful for describing photochemical degradations accompanied by fast reversible photoredox reactions, as should be the case for quinonoid compounds.

Acknowledgments

We thank Prof. U. P. Wild and Dr. A. Rebane for their support to this project, especially for giving us the opportunity to use the picosecond time-resolved fluorescence apparatus. S.C. and J.B.K. are grateful for financial support from Ciba-Geigy AG, Basel. We thank Dr. R. Hochberg and Dr. J. Kaschig for providing the FWAs and for their various contributions to this work. We also thank Dr. M. Elovitz for critically reading the manuscript and Prof. J. Hoigné, Prof. W. Giger, Dr. R. Hilfiker, Prof. J. Saltiel, and Dr. H. Görner for helpful discussions and suggestions.

Supporting Information Available

Two tables giving the fluorescence lifetimes and $\phi_{E,iso}/\phi_{Z,iso}$ of the FWAs at various temperatures and 1 page of text giving the simultaneous data fit of fluorescence lifetimes and photoisomerization quantum yield ratios of FWAs (3 pp) will appear following these pages in the microfilm edition of this volume of the journal. Photocopies of the Supporting Information from this paper or microfiche (105 × 148 mm, 24× reduction, negatives) may be obtained from Microforms Office, American Chemical Society, 1155 16th St. NW,

Washington, DC 20036. Full bibliographic citation (journal, title of article, names of authors, inclusive pagination, volume number, and issue number) and prepayment, check or money order for $12.00 for photocopy ($14.00 foreign) or $12.00 for microfiche ($13.00 foreign), are required. Canadian residents should add 7% GST. Supporting Information is also available via the World Wide Web at URL http://www.chemcenter.org. Users should select Electronic Publications and then Environmental Science and Technology under Electronic Editions. Detailed instructions for using this service, along with a description of the file formats, are available at this site. To download the Supporting Information, enter the journal subscription number from your mailing label. For additional information on electronic access, send electronic mail to si-help@acs.org or phone (202)872-6333.

Literature Cited

(1) Kramer, J. B. In *The Handbook of Environmental Chemistry*; Hutzinger, O., Ed.; Part 3F; de Oude, N., Ed.; Springer: New York, 1992; pp 351−366.
(2) Poiger, T.; Field, J. A.; Field, T. M.; Giger, W. *Anal. Methods Instrum.* **1993**, *1*, 104−113.
(3) Anliker, R.; Müller, G. In *Fluorescent Whitening Agents;* Coulston, F., Korte, F., Eds.; Environmental Quality and Safety Vol. IV; Thieme Verlag: Stuttgart, 1975.
(4) Kramer, J. B.; Canonica, S.; Hoigné, J.; Kaschig, J. *Environ. Sci. Technol.* **1996**, *30*, 2227−2234.
(5) Poiger, T.; Field, J. A.; Field, T. M.; Giger, W. *Environ. Sci. Technol.* **1996**, *30*, 2220−2226.
(6) Meier, H. *Angew. Chem.* **1992**, *104*, 1425−1576.
(7) Hilfiker, R. Private communication, Ciba-Geigy AG, Basel, 1996.
(8) Smit, K. J.; Ghiggino, K. P. *Dyes Pigm.* **1987**, *8*, 83−97.
(9) Rau, H. In *Photochromism. Molecules and Systems*; Dürr, H., Bouas-Laurent, H., Eds.; Studies in Organic Chemistry, Vol. 40; Elsevier: Amsterdam, 1990; pp 165−192.
(10) Saltiel, J.; Sun, Y.-P. In *Photochromism. Molecules and Systems*; Dürr, H., Bouas-Laurent, H., Eds.; Studies in Organic Chemistry, Vol. 40; Elsevier: Amsterdam; 1990; pp 64−164.
(11) Fleming, G. R. *Chemical Applications of Ultrafast Spectroscopy*; Oxford University Press: New York, 1986; p 179 ff.
(12) Waldeck, D. H. *Chem. Rev.* **1991**, *91*, 415−436.
(13) Todd, D. C.; Fleming, G. R. *J. Chem. Phys.* **1993**, *98*, 269−279.
(14) Görner, H.; Kuhn, H. J. *Adv. Photochem.* **1995**, *19*, 1−117.
(15) Repinec, S. T.; Sension, R. J.; Szarka, A. Z.; Hochstrasser, R. M. *J. Phys. Chem.* **1991**, *95*, 10380−10385.
(16) Canonica, S.; Forrer, J.; Wild, U. P. *Rev. Sci. Instrum.* **1985**, *56*, 1754−1758.
(17) Wild, U. P.; Holzwarth, A. R.; Good, H. P. *Rev. Sci. Instrum.* **1977**, *48*, 1621−1627.
(18) Smit, K. J.; Ghiggino, K. P. *Dyes Pigm.* **1990**, *13*, 45−53.
(19) Zepp, R. G.; Cline, D. M. *Environ. Sci. Technol.* **1977**, *11*, 359−366.
(20) Haag, W. R.; Hoigné, J. *Environ. Sci. Technol.* **1986**, *20*, 341−348.

Received for review September 3, 1996. Revised manuscript received January 21, 1997. Accepted January 28, 1997.[⊗]

ES960748A

[⊗] Abstract published in *Advance ACS Abstracts,* April 1, 1997.